Mine Classification based on a Fuzzy Characterisation

Isabelle Quidu, Jean-Philippe Malkasse, Pierre Vilbé, Gilles Burel

▶ **To cite this version:**

Isabelle Quidu, Jean-Philippe Malkasse, Pierre Vilbé, Gilles Burel. Mine Classification based on a Fuzzy Characterisation. Undersea Defence Technology (UDT) Europe 2002, Jun 2002, La Spezia, Italy. ⟨hal-00504850⟩

HAL Id: hal-00504850

https://hal.science/hal-00504850v1

Submitted on 21 Jul 2010

HAL is a multi-disciplinary open access archive for the deposit and dissemination of scientific research documents, whether they are published or not. The documents may come from teaching and research institutions in France or abroad, or from public or private research centers.

L'archive ouverte pluridisciplinaire **HAL**, est destinée au dépôt et à la diffusion de documents scientifiques de niveau recherche, publiés ou non, émanant des établissements d'enseignement et de recherche français ou étrangers, des laboratoires publics ou privés.

HAL Authorization

Mine Classification based on a Fuzzy Characterisation

I. Quidu[*], J. Ph. Malkasse[*], P. Vilbé[**], G. Burel[**]

(*) Thales Underwater Systems S.A.S., Route de Sainte Anne du Portzic, 29601 BREST cédex, France
isabelle.quidu@fr.thalesgroup.com, jean-philippe.malkasse@fr.thalesgroup.com
(**) L.E.S.T. - FRE CNRS 2269, 6 avenue Le Gorgeu, BP 809, 29285 BREST cédex, France
Pierre.Vilbe@univ-brest.fr, Gilles.Burel@univ-brest.fr

Abstract - High resolution sonars provide high-quality acoustic images, allowing the classification of objects from their cast shadow. For a given ground mine except mine with radial symmetry, shadow appearance generally depends on the point of view. After a segmentation step performed on images acquired along a part of a circular trajectory of the sonar around the object, we can match and superimpose binary data. The resulting image displays a fuzzy shadow region whose pixels grey-levels depend on their successive localisation in the images of the sequence, i.e. if they belong or not to the shadow region. As an extension of feature extraction in the binary case, fuzzy geometry is a practical tool to describe fuzzy regions characterised by the degree of membership of each pixel to them. After a Principal Component Analysis applied to a set of fuzzy features, encouraging results have been achieved on simulated sonar images covering both classical and stealthy mines.

I. Introduction

Fuzzy image processing consists in applying fuzzy logic to develop new image processing algorithms. Many classical image processing algorithms can be extended to fuzzy image processing algorithms (1). Fuzzy techniques are often used to manage uncertainties within image processing due to vagueness and ambiguity. Representation of image regions as fuzzy subsets seems to be well appropriate for our specific aim. Indeed, we do not deal with regions crisply defined but regions characterised by the degree of membership of each pixel to them. The idea we developed in this paper is to summarise in a single image all the sonar data acquired along a part of a semicircular trajectory of the sonar around the object and, to extend the classical features extraction step to characterise a new fuzzy shadow region whose pixels grey-levels depend on their successive localisation in the images of the sequence. It requires four preliminary steps we explain in the second section: a segmentation step, a superimposition step, a fuzzification step and an image normalisation. Rosenfeld generalised many basic geometrical properties of regions such as area, perimeter, height, length, compactness and so on, to fuzzy sets (2). Some of them are used here and specified in section III in conjunction with new fuzzy features we derived. In section V, a Principal Component Analysis is applied to a large set of fuzzy features described in section IV.

II. Preliminary steps

Before defining the features, we explain how image data are preprocessed in order to obtain a fuzzy region. Without further details at this point, we only suppose that we deal with a sequence of N_v different points of view per object to be classified. Details about conditions of simulations will be explained later in section V. Figure 1, Figure 2 and Figure 3 illustrate the following steps that enable us to obtain the fuzzy image.

II.1. Segmentation step (cf. Figure 1)

Segmentation consists in partitioning the image into homogeneous regions. In our case, objects are classified from their cast shadow. Each image is made up of both the echo and the cast shadow caused by the detected object and the seabed reverberation region. Giving the label zero for pixels belonging to the shadow and the label one elsewhere we obtain binary from grey-level image. Sonar image's grey-level histogram is generally unimodal and then threshold selection by the mode method is impossible. To make it bimodal, a specific spatial filtering can be applied in order to minimise pixels variance. In the resulting histogram, peaks represent shadow and seabed reverberation regions (differing in average grey-level) while the single valley represents shadow edge. The optimal filter designed for sonar images does not look like a classic low-pass filter but strongly depends on the principle of the sonar image formation in terms of size and coefficient values. For details on this technique, please refer to (3).

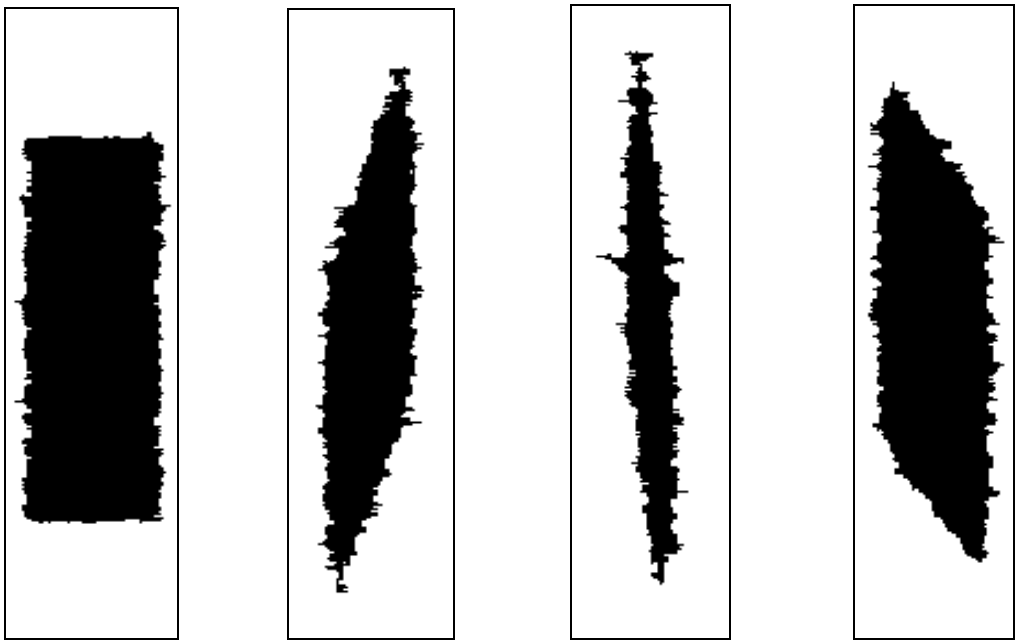

Figure 1 –Images segmentation over a sequence of cylinder cast shadows (only four of them are displayed here)

II.2. Superimposition step (cf. Figure 2)

By superimposing all the segmented shadows of the sequence, we observe straight on a single image different shapes of shadow that the object can cast. Necessarily, superposition is carried out after the centres of mass of the shapes have been fitted. As a result, the more shapes differ, the more the dispersion of pixels levels is important because pixel level depends on its successive localisation in the images of the sequence, i.e. if it belongs or not to the shadow region. Using N_v images, the maximal pixel grey-level is N_v.

II.3. Fuzzification step (cf. Figure 2)

Fuzzy logic seems to be appropriate to characterise the new image provided that a fuzzification is operated. It means that we assign the image with membership values regarding to pixels belongness to the shadow region over the sequence. In order to affect the maximal membership value at the centre of the fuzzy region and zero for pixels that never belong to the shadow region over the sequence, we invert grey-levels. By normalising each pixel grey-level by the maximal one, we transform the region of interest into a fuzzy subset of the image where for every pixel p whose coordinates are (i, j), $\mu(p) = \mu(i, j)$ is called the degree of membership of p in μ, a mapping from the image into [0,1].

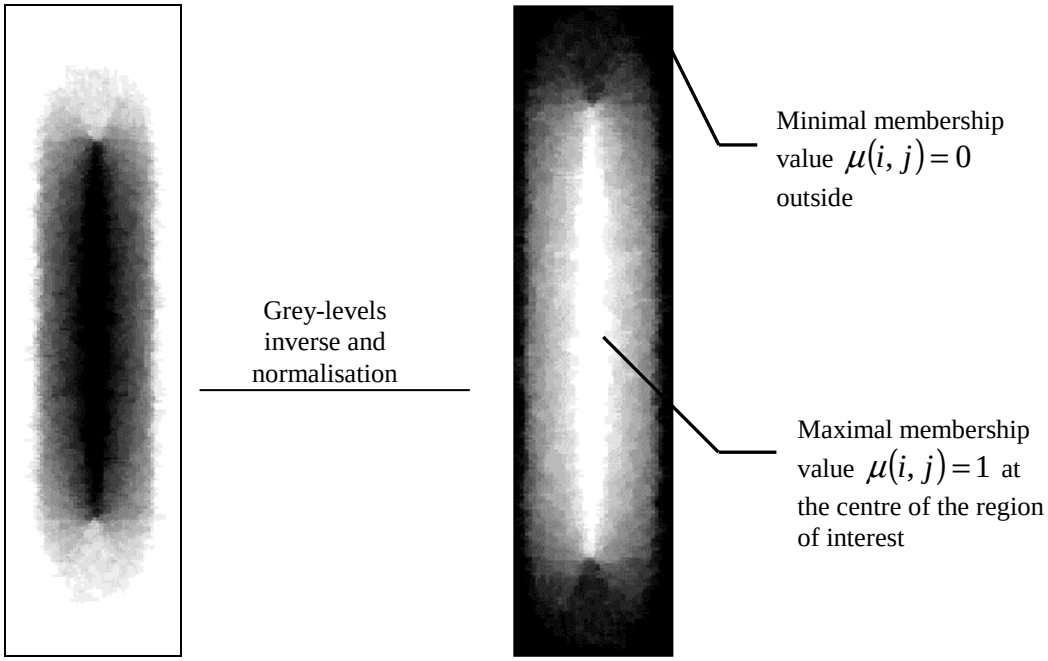

Figure 2 –Superimposition, pixels levels inverse and fuzzification

II.4. Image normalisation (cf. Figure 3)

To improve robustness of features, an image normalisation is performed. It has to provide a new image as if it would be seen under a grazing angle of 45 degrees preserving shadow ratios. Moreover on account of the sonar parameters, image resolution is generally different along the two dimensions. Consequently, each pixel is made approximately "square" to prevent from disproportions.

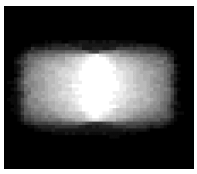

Figure 3 – Image normalisation

III. Fuzzy features

The feature extraction step is a process by which the previous grey-level images are transformed into a pattern feature vector.

III.1. Rosenfeld geometrical features

Among the geometrical features introduced by Rosenfeld and extended by Pal and Ghosh, we were interested in the following ones (in case of digital image, where *i* stands for index of row and *j* for index of column) (2)(4):

- area a

$$a(\mu) = \sum_i \sum_j \mu(i, j)$$

- height h

$$h(\mu) = \sum_j \max_i \{\mu(i, j)\}$$

- width w

$$w(\mu) = \sum_i \max_j \{\mu(i, j)\}$$

- length l

$$l(\mu) = \max_i \sum_j \mu(i, j)$$

- breath L

$$L(\mu) = \max_j \sum_i \mu(i, j)$$

By combining the previous features, we can also evaluate:

- Index of area coverage $IOAC$

$$IOAC(\mu) = \frac{a(\mu)}{L(\mu) \times l(\mu)}$$

In the nonfuzzy case, this feature equals to 1 for a rectangle placed along the axes of the image and $\pi/4$ for a circle.

- Density d

$d(\mu) = \dfrac{a(\mu)}{N}$ where *N* stands for the number of pixels whose membership values differ from zero

III.2. Fuzzy features derived from fuzzy moments

a) Fuzzy moments

The two-dimensional moment of order $p+q$ for an $(N \times M)$ discretized image, $f(i, j)$ is defined as (5):

$$m_{pq} = \sum_{j=0}^{M-1} \sum_{i=0}^{N-1} i^p j^q f(i, j)$$

Moments are usually applied to a distribution function that is binary and contiguous, i.e. a silhouette image of a segmented object (shadow in our case) to extract shape characteristics. The extent of moments in the fuzzy case is straightforward:

$$\tilde{m}_{pq} = \sum_{j=0}^{M-1} \sum_{i=0}^{N-1} i^p j^q \mu(i, j)$$

We easily derive the corresponding fuzzy central moments:

$$\tilde{m}'_{pq} = \sum_{j=0}^{M-1} \sum_{i=0}^{N-1} (i - i_0)^p (j - j_0)^q \mu(i, j) \text{ with } i_0 = \frac{\tilde{m}_{10}}{\tilde{m}_{00}} \text{ et } j_0 = \frac{\tilde{m}_{01}}{\tilde{m}_{00}}$$

b) New fuzzy geometrical features

As an extension to fuzzy sets, we can now introduce the following features that have been successfully used in the binary case (6) :

- Extent *Et*

$$Et(\mu) = \frac{\tilde{m}'_{20} + \tilde{m}'_{02}}{\tilde{m}'^2_{00}}$$

- Elongation *El*

$$El_1(\mu) = \frac{\sqrt{4\tilde{m}'^2_{11} + (\tilde{m}'_{20} - \tilde{m}'_{02})^2}}{\tilde{m}'_{20} + \tilde{m}'_{02}} \text{ or } El_2(\mu) = \frac{\alpha}{\beta}$$

where

$$\begin{cases} \alpha = \sqrt{\dfrac{2\left[\tilde{m}'_{20} + \tilde{m}'_{02} + \sqrt{(\tilde{m}'_{20} - \tilde{m}'_{02})^2 + 4\tilde{m}'^2_{11}}\right]}{\tilde{m}'_{00}}} \\ \beta = \sqrt{\dfrac{2\left[\tilde{m}'_{20} + \tilde{m}'_{02} - \sqrt{(\tilde{m}'_{20} - \tilde{m}'_{02})^2 + 4\tilde{m}'^2_{11}}\right]}{\tilde{m}'_{00}}} \end{cases}$$

- Intensity of the image *Ellipse*

$$Ellipse(\mu) = \frac{\tilde{m}'_{00}}{\pi\alpha\beta}$$

IV. Fuzzy features extraction

As in the binary case, if we except the index of area coverage, geometrical features differ within a given class, depending on size. It results a partition within some classes. In such a case, the k-nearest-neighbour algorithm can be used to avoid misclassifications.

Without any *a priori* choice among all the previous fuzzy features, our feature vector is made of 9 components consisting in 9 geometrical features, i.e. *d*, *IOAC*, *Et*, El_2, *Ellipse*, *h*, *w*, *L*, *l*. In the remainder, we call *individual* a given fuzzy region described by its 9 features $(a_j)_{j \in \{1...9\}}$.

V. Experiments

V.1. Training set

Sonar data are simulated in order to cover a wide set of configurations in terms of types of mines and appearances from different points of view. On one hand, moored mines generally look like a sphere coupled to an anchor box for laying. On the other hand, ground mines are usually cylindrical in shape. Nevertheless while cylindrical shaped objects reflect fairly definite sonar shadows, some ground mines have specific shape that improves stealth capabilities resulting in a difficult identification (9). In our experiments, five classes have then been considered: cylinders (3 sizes), spheres (3 sizes), and three stealthy mines, i.e. two that look like truncated cones (the Manta and Sigeel mines) and another one with sloping angled faces and low profile (the Rockan mine). To achieve our experiments, a sequence of 19 sonar images is simulated per mine as if the sonar turned around each mine with a shot every 10 degrees. The entire training set is made of 270 sequences. Sonar height and distance from the sonar to the object are kept constant along the trajectory. These are realistic conditions if we use a sonar mounted on the Propelled Variable Depth Sonar (PVDS) promoted by Thales Underwater Systems that can easily work. Moreover synthetic aperture processing self-calibration enables us to know very precisely the trajectory, and, by means of small corrections, to get the required trajectory conditions back (10).

In order to evaluate the robustness of our features, we paid attention to two points:

- We do not *a priori* know the orientation of the object from the sonar: The superimposition of the segmented images is then performed from a random start of the trajectory. As a consequence, in case of a mine that has a single axis of symmetry (as the Rockan mine), the aspect of the fuzzy region differs according to the start point.
- The evolution of the classification results when we limit the semicircular trajectory to a quarter of a circular trajectory, i.e. 10 successive points of view.

Figure 4 (*resp.* Figure 5) displays an example of fuzzy regions obtained by the method explained above (section II) for each class when the superimposition step uses N_v=19 images (*resp.* N_v=10 images). As expected, regions obtained in case of mines with poor symmetrical properties such as cylinder or Rockan mine are fuzzier than those obtained in case of mines with radial symmetry. Effectively, the shadow cast by the firsts has different appearances with respect to the sonar observation viewpoint.

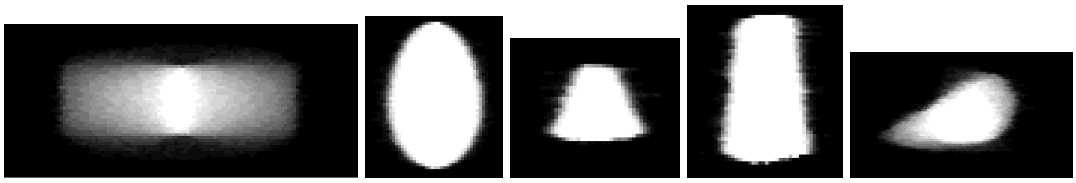

Figure 4 – Examples of fuzzy regions for different types of mines considering a semicircular trajectory : a cylinder, a sphere, a Manta mine, a Sigeel mine and a Rockan mine

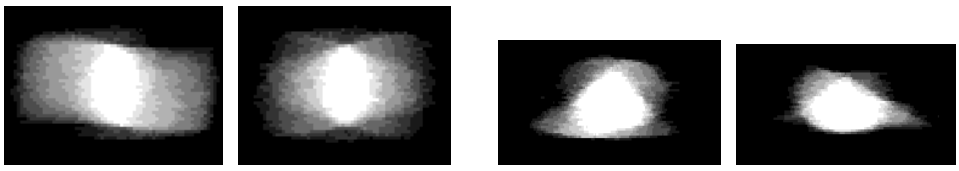

Figure 5 – Examples of fuzzy regions for different types of mines considering a quarter of a circular trajectory : 2 cylinders and 2 Rockan mines

V.2. Fuzzy features analysis

In order to analyse easily relevance of fuzzy features to our specific application, a Principal Component Analysis followed by a correlation circle interpretation are performed.

a) Principal Component Analysis (PCA)

PCA allows to reduce dimensionality by forming linear combinations of features while preserving the maximum of variance. It consists in finding the principal axes of inertia through the feature space and

projecting data along these axes. A covariance matrix $\frac{1}{N_b}CC^T$ of size 9×9 is then constructed from the set of the centred and reduced features (so that all the features have zero mean and unit variance) C of size $9\times N_b$ where N_b stands for the number of individuals (^{T} stands for the transpose operation) (7)(8). The principal axes are the eigenvectors of the covariance matrix associated to its eigenvalues. We can then visualise the best clustering in the feature space projecting the feature values on the base of the eigenvectors $U=(u_{ij}),(i,j)\in\{1,...,9\}\times\{1,...,9\}$.

As the features are centred and reduced, the total inertia I of the cluster of the whole individuals, i.e. the sum of the eigenvalues, is equal to the number of features, i.e. 9 (7). As the ratio $(\lambda_1+\lambda_2)/I$ is sufficient, i.e. the part of the inertia related to the two first principal axes, we can replace the features by the two first components only and reduce the size of the feature space from 9 to only two dimensions.

Doing the projection $F = U^T C$, we visualise the 2D-subspace $f_1 = f(f_2)$, where f_1 and f_2 are the two first lines of F and are related to the coordinates of the individuals in the principal plane. This plane is the best projection of the initial 9D-space when the 9 features $(a_j)_{j=1...9}$ are combined to compute two new synthetic features, i.e. the principal components f_1 and f_2. In other words, the principal plane can be seen as the plane that maximises the inertia of the individuals projected on it.

b) Correlation circle

To give an interpretation of the positions of the individuals in the principal plane, one can use the correlation circle of unit radius. On this graph, coordinates of each point stand for the correlation of each feature a_j with the two principal components f_1 and f_2. For our centred and reduced features, correlation is equal to $r(f_l,a_j)=u_{lj}\times\sqrt{\lambda_l}$ (7). The correlation circle creates a link between the two spaces by means of correlations. The more the features are characterised by a large radius $\sqrt{r^2(f_1,a_i)+r^2(f_2,a_i)}$, the more they are correlated with the principal components and then, discriminant for our application.

c) Experimental results

First case: a semicircular trajectory (19 points of view)

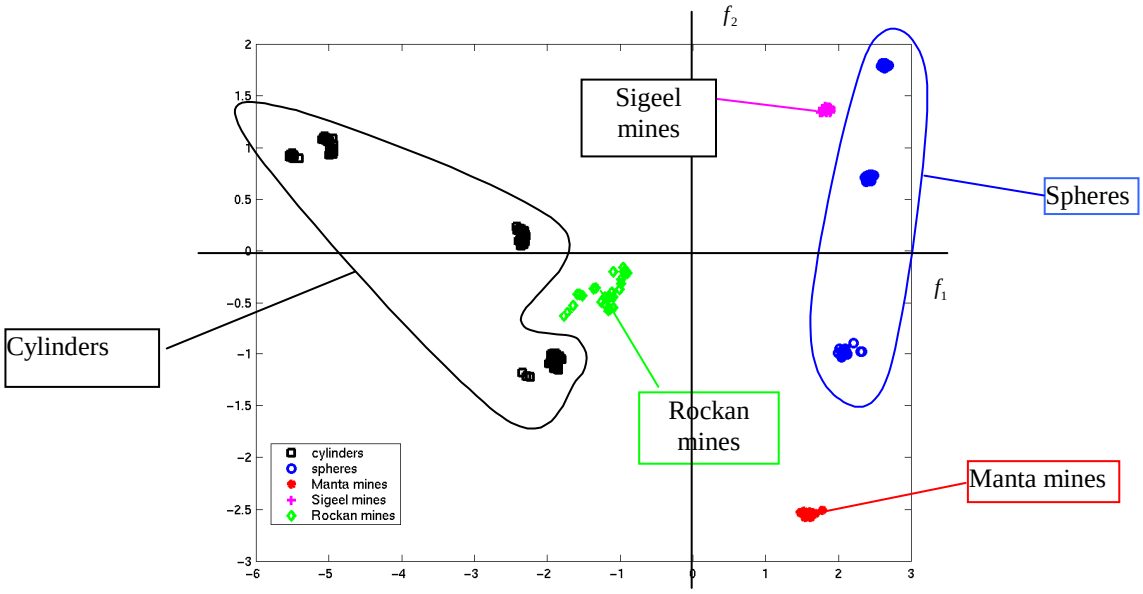

Figure 6 - Partition of the subspace in case of a semicircular trajectory: $(\lambda_1+\lambda_2)/I = 0.847$

As planned, more than a single cluster are assigned to individuals of classes 'cylinders' or 'spheres' because of their different possible sizes. Seeing the perfect partition of the individuals in this 2D-subspace, a K-nearest neighbour classifier with K=1 successfully provides 100% of good classification.

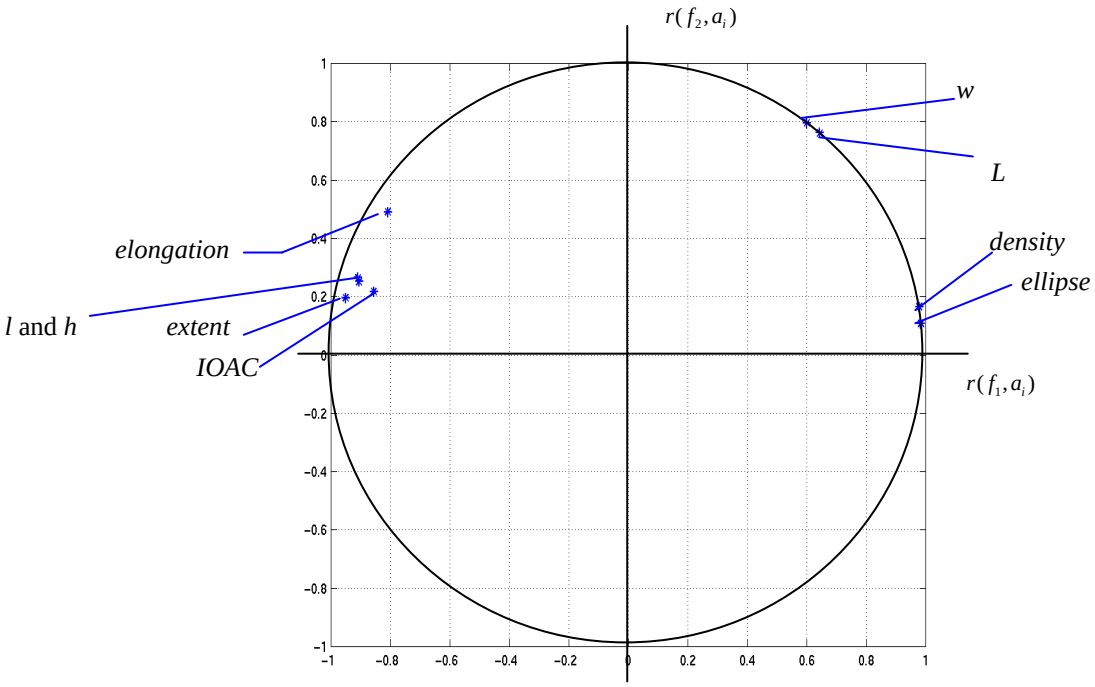

Figure 7 - Correlation circle in case of a semicircular trajectory

Seeing the correlation circle on Figure 7, we can give an interpretation of the partition of the individuals in the principal plane according to their symmetrical properties. The principal component f_1 separates objects with radial symmetry (i.e. Manta mines, Sigeel mines and spheres) from the others (i.e. cylinders and Rockan mines). Indeed, features sensitive to fuzziness, such as *density* and *ellipse*, are the most correlated with it.

Second case: a quarter of a circular trajectory (10 points of view)

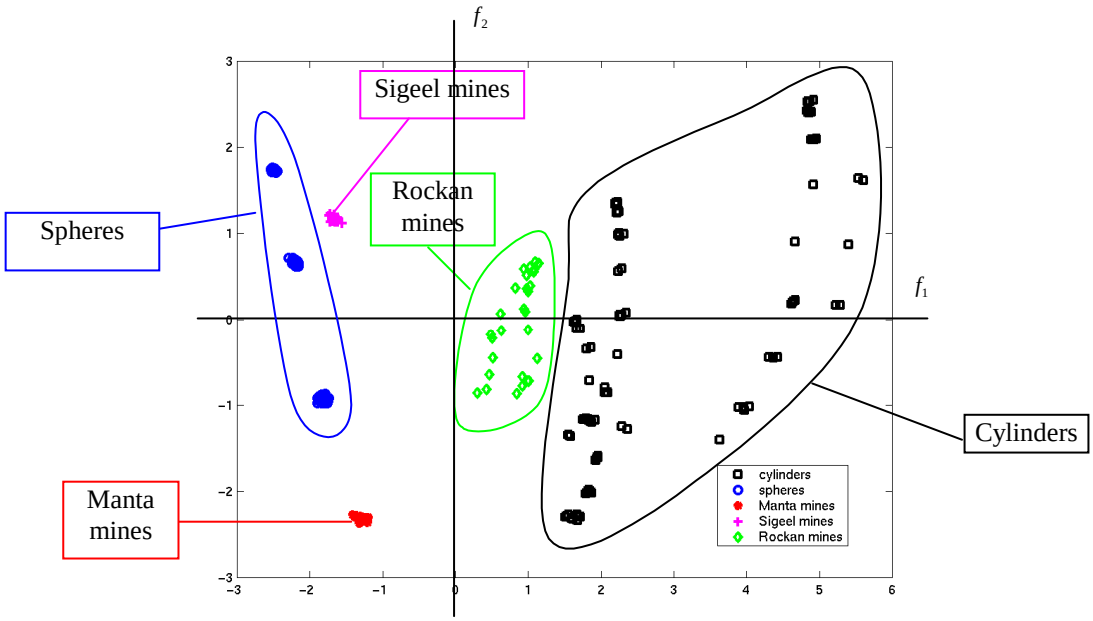

Figure 8 - Partition of the subspace in case of a quarter of a circular trajectory: $(\lambda_1 + \lambda_2)/I = 0.836$

With regard to the previous case, individuals related to classes ‘ cylinders’ and ‘ Rockan mines’ are more spread. Their complex symmetry entails a large number of possible aspects of the fuzzy region. Nevertheless, a K-nearest neighbour classifier with K=1 still provides 100% of good classification.

VI. Conclusion

In this paper, we have shown the interest of the extension of the classical features extracted from binary 2D-shape to fuzzy features extracted from fuzzy 2D-shape to perform a new recognition processing over a sequence of images of the same object. Actually, a single image created from all the segmented images of the sequence displays a new region of interest with a fuzzy frontier. The more the number of segmented images is large, the less a possible bad segmentation (noisy or partially hidden shadow) has a consequence on the classification. Very encouraging results have been achieved and show that fuzzy geometry is a relevant tool to deal with such data.

As an alternative, we can plan to superimpose raw data. But, as mentioned in the recent thesis (11), that entails some difficulties to make shadows coincide with each others. Furthermore, we have to discard pixels that belong to the seabed reverberation area so as to they do not interfere in the computation of fuzzy features.

VII. References

(1) H.R. Tizhoosh; Fuzzy Image Processing: Potentials and State of the Art; 1998; Proceedings of IIZUKA'98, pp. 321-324.

(2) A. Rosenfeld; The fuzzy geometry of image subsets; 1984; Pattern Recognition Letters, vol. 2, pp. 311-317.

(3) I. Quidu, J.P. Malkasse, G. Burel and P. Vilbé; A 2-D Filter Specification for Sonar Image Thresholding; 2001; Advanced Concepts for Intelligent Vision Systems (ACIVS'2001) conference, Baden-Baden, Germany.

(4) S.K. Pal and A. Ghosh; Fuzzy geometry in image analysis; Fuzzy Sets and Systems; 1992; vol. 48, pp. 23-40.

(5) R.J. Prokop and A.P. Reeves; A Survey of Moment-Based Techniques for Unoccluded Object Representation and Recognition; 1992; CVGIP: Graphical Models and Image Processing, vol. 54, No. 5, pp. 438-460.

(6) I. Quidu, J.P. Malkasse, G. Burel and P. Vilbé ; Mine classification using a hybrid set of descriptors ; 2000 ; Proceedings of OCEANS'2000 MTS/IEEE, Providence, Rhode Island.

(7) J.M. Bouroche and G. Saporta ; *L'analyse des données*, Collection "Que sais-je ? ", Presses Universitaires de France ; 1998.

(8) M. Volle ; *Analyse de données*, Economica, 3ième éd. ; 1985.

(9) *Jane's Underwater Warfare Systems*, Ed. By Anthony J. Watts, Tenth Edition 1998-1999.

(10) D. Billon and F. Fohanno ; Theoretical performance and experimental results for synthetic aperture sonar self-calibration ; *Proc. OCEANS'98 MTS/IEEE*, Nice, France ; pp. 965-970 ; 1998.

(11) I. Quidu ; Classification multi-vues d'un objet immergé à partir d'images sonar et de son ombre portée sur le fond ; PhD Thesis, Université de Bretagne Occidentale, France ; 2001.